PHYSICAL REVIEW B **96**, 104502 (2017)

Spin-singlet superconductivity in the doped topological crystalline insulator $Sn_{0.96}In_{0.04}Te$

Satoki Maeda,[1] Ryohei Hirose,[1] Kazuaki Matano,[1] Mario Novak,[2] Yoichi Ando,[3] and Guo-qing Zheng[1,4]
[1]*Department of Physics, Okayama University, Okayama 700-8530, Japan*
[2]*Institute of Scientific and Industrial Research, Osaka University, Osaka 567-0047, Japan*
[3]*Physics Institute II, University of Cologne, Köln 50937, Germany*
[4]*Institute of Physics, Chinese Academy of Sciences, and Beijing National Laboratory for Condensed Matter Physics, Beijing 100190, China*
(Received 22 May 2017; published 5 September 2017)

The In-doped topological crystalline insulator $Sn_{1-x}In_xTe$ is a candidate for a topological superconductor, where a pseudo-spin-triplet state has been proposed. To clarify the spin symmetry of $Sn_{1-x}In_xTe$, we perform ^{125}Te-nuclear magnetic resonance (NMR) measurements in polycrystalline samples with $0 \leqslant x \leqslant 0.15$. The penetration depth calculated from the NMR line width is T independent below half the superconducting transition temperature (T_c) in polycrystalline $Sn_{0.96}In_{0.04}Te$, which indicates a fully opened superconducting gap. In this sample, the spin susceptibility measured by the spin Knight shift (K_s) at an external magnetic field of $\mu_0 H_0 = 0.0872$ T decreases below T_c, and $K_s(T=0)/K_s(T=T_c)$ reaches 0.36 ± 0.10, which is far below the limiting value 2/3 expected for a spin-triplet state for a cubic crystal structure. Our result indicates that polycrystalline $Sn_{0.96}In_{0.04}Te$ is a spin-singlet superconductor.

DOI: 10.1103/PhysRevB.96.104502

I. INTRODUCTION

Topological insulators (TIs) and topological crystalline insulators (TCIs) are materials in which the bulk is insulating but the surface hosts metallic states due to nonzero topological invariants of the bulk band structure [1–5]. A TI requires time-reversal symmetry, while a TCI requires certain symmetries in crystal structure such as mirror symmetry. Recently, superconductivity realized in carrier-doped TIs or TCIs has attracted great interest, as it can be topological. A topological superconductor is analogous to TI or TCI in that the superconducting gap function has a nontrivial topological invariant [2,6,7]. Vast efforts have been devoted to establishing topological superconductivity with time-reversal symmetry in a bulk material, but the progress had been slow until the recent discovery of a pseudo-spin-triplet, odd-parity superconducting state [8] in the doped TI, $Cu_xBi_2Se_3$ [9].

SnTe with NaCl-type crystal structure is a TCI [3,4] and shows superconductivity upon Sn vacancies or In doping [10–12]. A quasilocalized impurity bound state due to In doping was recently evidenced by ^{125}Te-NMR measurements [13], which forms the background electronic state responsible for superconductivity [14,15]. Point-contact spectroscopy performed on clean single crystals of $Sn_{0.955}In_{0.045}Te$ found a zero-bias conductance peak, which was taken as a signature of unconventional superconductivity [16]. Specific heat [17], thermal conductivity [18], and μSR [19] have revealed a fully opened superconductiviting gap. Combining these results, a fully gapped pseudo-spin-triplet state was theoretically proposed [20]. However, since the spin symmetry of Cooper pairs is unexamined, Knight-shift measurements by nuclear magnetic resonance (NMR) that can probe the spin susceptibility below T_c are highly desired.

In metals, the Knight shift (K) contains two contributions as $K = K_{chem} + K_s$, where K_{chem} is the chemical shift, which is composed of contributions due to orbital susceptibility and diamagnetic susceptibility of closed inner shells, and K_s is due to spin susceptibility. The temperature variation of K_s below T_c depends on the spin symmetry of the Cooper pairs. For a spin-singlet superconductor with a weak spin-orbit interaction, K_s decreases below T_c and vanishes at $T = 0$ K. On the other hand, the K_s of a spin-triplet superconductor depends on the detail of the d vector that describes the paired spins. The d vector is perpendicular to the plane in which the parallel spins lie, and when this vector is pinned to a special direction of the lattice, the K_s is invariant across T_c for a magnetic field applied perpendicular to the d vector, while it decreases for a magnetic field parallel to the d vector. This was indeed observed for the first time in $Cu_xBi_2Se_3$ [8]. For the fully gapped spin-triplet state proposed for $Sn_{1-x}In_xTe$ [20], K_s will decrease in a certain direction if the spins are well fixed to the lattice, as in $Cu_xBi_2Se_3$ [8]. In the case of polycrystalline samples with a cubic structure, where K_s is an average over all directions, at most one-third of the K_s can be reduced at $T = 0$. Therefore, measurement of the temperature variation of K_s allows one to determine the spin pairing symmetry.

In this paper, we report ^{125}Te-NMR measurements of polycrystalline $Sn_{1-x}In_xTe$. First, we determine the quantity K_{chem} using the relationship between K and the spin-lattice relaxation time (T_1) of $Sn_{1-x}In_xTe$ with various x's. Then we measured the K_s for $Sn_{0.96}In_{0.04}Te$ down to $T = 0.1$ K under the very small magnetic field of $\mu_0 H_0 = 0.0872$ T. The obtained result indicates a spin-singlet pairing.

II. EXPERIMENTAL PROCEDURE

Polycrystalline samples of $x = 0$, 0.05, 0.1, and 0.15 were synthesized by a sintering method at Okayama as described in the previous paper [13]. An effectively polycrystalline sample of $x = 0.04$ was synthesized by a melt-growth technique at Osaka. This sample was initially attempted to be grown as a big single crystal, but Laue diffraction showed that it consists of many crystallites. The T_c was determined by measuring the inductance of the NMR coil. NMR measurements were carried out using a phase-coherent spectrometer. NMR spectra under an external magnetic field $\mu_0 H_0 = 5$ T were obtained by integrating the spin-echo intensity by changing the resonance frequency (f). In order to minimize the reduction of T_c by

the applied field, most of the measurements for $x = 0.04$ were performed at the small field of $\mu_0 H_0 = 0.0872$ T, under which the NMR spectra were obtained by a fast Fourier transform of the spin echo. T_1 was measured using a single saturating pulse and determined by fitting the recovery curve of the nuclear magnetization to a single exponential function, $(M_0 - M(t))/M_0 = \exp(-t/T_1)$, where M_0 and $M(t)$ are the nuclear magnetization in the thermal equilibrium and at time t after the saturating pulse. Measurements below 1.4 K were carried out with a ^{3}He-^{4}He dilution refrigerator. After completion of all the NMR measurements, the large sample of $x = 0.04$ was crushed into several pieces and Hall coefficient measurements were performed on them. The Hall coefficient shows a distribution of 30% from piece to piece, but the averaged value indicates that the averaged x over the sample is 0.04.

III. RESULTS

We first explain how we obtained $K_{\rm chem}$. In a normal metal, both $K_{\rm s}$ and the quantity $(T_1T)^{-1/2}$ are proportional to the density of states at the Fermi level [$N(E_F)$], and $K_{\rm s}$ and T_1 satisfy the Korringa relation $T_1 T K_{\rm s}^2 = \frac{\hbar}{4\pi k_B}(\frac{\gamma_e}{\gamma_n})^2$, where $\gamma_{e(n)}$ is the gyromagnetic ratio of the electron (nucleus). This was recently found to be true in this system under a relatively high field ($\mu_0 H_0 = 5$ T) [13]. The inset in Fig. 1 shows the x dependence of the K and $(T_1T)^{-1/2}$ measured at the peak position of the spectrum. K and $(T_1T)^{-1/2}$ increased with an increase in x, which means an increase in $N(E_{\rm F})$ with increasing x. As shown in Fig. 1, K and $(T_1T)^{-1/2}$ show a good linear relationship with x as an implicit parameter. Thus $K_{\rm chem}$ can be determined as an intercept in a K-$(T_1T)^{-1/2}$ plot. As shown in Fig. 1, by extrapolating the data to the origin, where $(1/T_1T)^{-1/2} = 0$, $K_{\rm chem} = -0.293 \pm 0.005\%$ is obtained. The negative value of $K_{\rm chem}$ is due to the large diamagnetism of the inner shells.

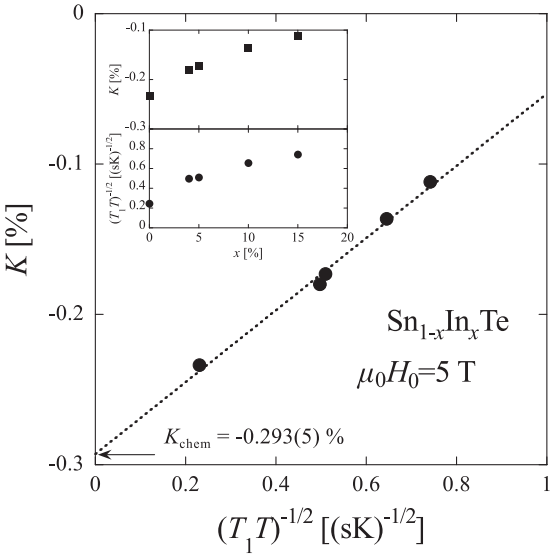

FIG. 1. K-$(T_1T)^{-1/2}$ plot for various x's under $\mu_0 H_0 = 5$ T. Inset: The x dependence of the K and $(T_1T)^{-1/2}$ measured at the peak position of the spectrum. Smooth evolution of the two physical quantities indicates that the real doping level changes smoothly with x.

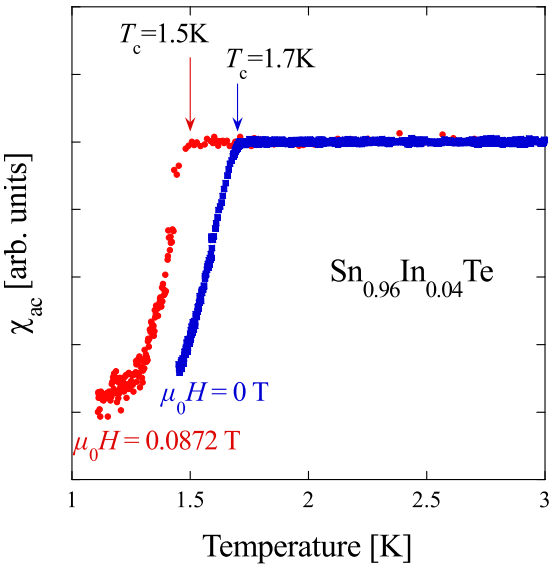

FIG. 2. Temperature dependence of the $\chi_{\rm ac}$ for $Sn_{0.96}In_{0.04}Te$ at $\mu_0 H = 0$ and 0.0872 T.

Next, we discuss the result in the superconducting state. Figure 2 shows the temperature dependence of the ac susceptibility ($\chi_{\rm ac}$) for $Sn_{0.96}In_{0.04}Te$, which showed superconductivity at 1.7 K under $\mu_0 H_0 = 0$ T and at 1.5 K under $\mu_0 H_0 = 0.0872$ T. The T_c at $H_0 = 0$ T was significantly higher than the reported value for $x \sim 0.04$ [16,21], which is commented on later. It is reported that the upper critical field H_{c2} for $Sn_{1-x}In_xTe$ with a high In content is well fitted by the parabolic formula [19], $H_{c2}(T) = H_{c2}(0)[1 - (T/T_c)^2]$. Using this relation, $\mu_0 H_{c2} = 0.43$ T is obtained. On the other hand, using the Werthamer-Helfand-Hohenberg theory [22], $\mu_0 H_{c2} = 0.53$ T is obtained from the initial slope of H vs T_c.

Figure 3 shows the temperature dependence of the ^{125}Te-NMR spectrum for $Sn_{0.96}In_{0.04}Te$ under $\mu_0 H_0 = 0.0872$ T.

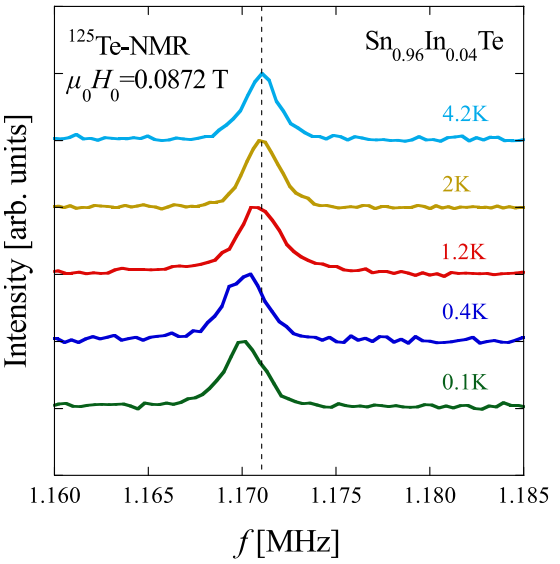

FIG. 3. ^{125}Te-NMR spectra for $Sn_{0.96}In_{0.04}Te$ at various temperatures under $\mu_0 H_0 = 0.0872$ T.

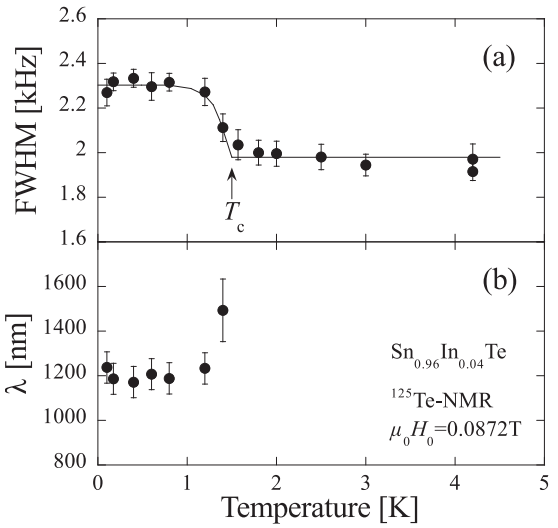

FIG. 4. (a) Temperature dependence of the FWHM for $Sn_{0.96}In_{0.04}Te$ under $\mu_0 H_0 = 0.0872$ T. The curve is a guide for the eye. (b) Temperature dependence of the penetration depth λ calculated from the FWHM.

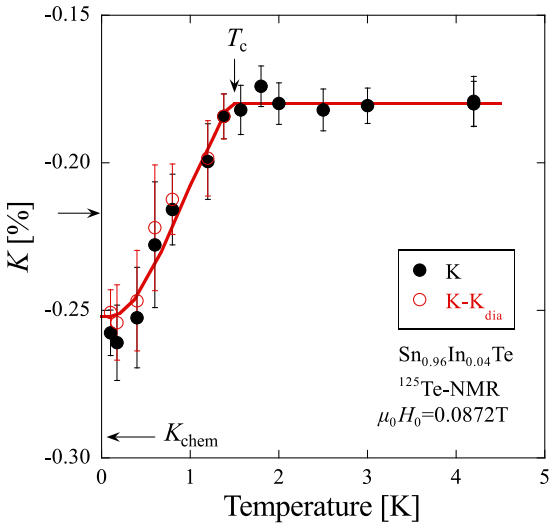

FIG. 5. Temperature dependence of the Knight shift K and the corrected value $K - K_{dia}$ for $Sn_{0.96}In_{0.04}Te$ under $\mu_0 H_0 = 0.0872$ T. The upper arrow indicates the position for the case where one-third of the K_s is reduced, and the lower arrow indicates the position of K_{chem} ($K_s = 0$). The curve is a guide for the eye.

The peak is temperature independent above $T_c(H) = 1.5$ K but shifts to a lower frequency with decreasing temperature. Figure 4(a) shows the temperature dependence of the full width at half-maximum (FWHM). The FWHM increases below T_c, due to a magnetic-field distribution in the vortex state. It is related to the penetration depth (λ) as [23]

$$\sqrt{\mathrm{FWHM}^2(T) - \mathrm{FWHM}^2(T_c)} = 0.0609\gamma_n \frac{\phi_0}{\lambda^2(T)}. \quad (1)$$

$\lambda(T = 0) \sim 1200$ nm was obtained from the above equation, which is larger than the $\lambda = 542$ nm reported by muon-spin spectroscopy for a sample with a higher In concentration ($x = 0.4$, $T_c = 4.69$ K) [19]. Since the λ is proportional to the carrier concentration n as $-1/2$ ($\lambda \propto n^{-1/2}$) [24], the difference in λ between $x = 0.04$ and $x = 0.4$ is most likely due to the difference in carrier concentration.

As shown in Fig. 4(b), λ is T independent below 0.5 T_c, which indicates that the superconducting gap is fully opened. In a superconductor with nodes, λ is proportional to T^n ($n \geqslant 1$) at low temperatures. Our result is consistent with the specific heat [17], thermal conductivity [18], and μSR [19] measurements in $Sn_{1-x}In_xTe$ and the scanning tunneling spectroscopy in $(Pb_{0.5}Sn_{0.5})_{0.7}In_{0.3}Te$ [25].

Figure 5 shows the temperature dependence of the Knight shift K, which is T independent above T_c but decreases below T_c. In the vortex state, one needs to consider a diamagnetic shift K_{dia} (<0) arising from an inhomogeneous field distribution due to the formation of vortex lattices. Namely, the magnetic field is position dependent within the sample, which can be smaller than the applied field in some positions. The position-dependent field $h(\boldsymbol{r})$ is calculated using the London model [26],

$$h(\boldsymbol{r}) = H \sum_{l,m} \frac{\exp\left(-G_{lm}^2\xi^2/2\right)\exp(-i\boldsymbol{G}_{lm}\cdot\boldsymbol{r})}{1 + G_{lm}^2\lambda^2}, \quad (2)$$

$$\boldsymbol{G}_{lm} = 2\pi\sqrt{\frac{H\sin(\beta)}{\phi_0}}\left\{m\boldsymbol{x} + \frac{l - m\cos(\beta)}{\sin(\beta)}\boldsymbol{y}\right\}, \quad (3)$$

where H is the applied field and ξ is the coherence length. The summation runs over all reciprocal vortex lattices $\boldsymbol{G}_{lm}$, where $\boldsymbol{x}$ and $\boldsymbol{y}$ are the unit vectors of the vortex lattices, and β is the angle between two primitive vortex lattice vectors. We assumed $\beta = 60^\circ$ and that ξ and λ are isotropic, reflecting the cubic crystal structure. The density function of the magnetic field is obtained as $f(h) = \int \delta(h - h(\boldsymbol{r}))d^3\boldsymbol{r}$. K_{dia} was determined using the peak position of the convolution of the $f(h)$ and the spectrum in the normal state approximated by a Gaussian function. We used $\mu_0 H_{c2} = 0.43$ T, which gives $\xi = 27.7$ nm from the relation $H_{c2} = \phi_0/2\pi\xi^2$ [24]. The open circles in Fig. 5 show the corrected Knight shift $K - K_{dia}$. In the figure, the position of $K_{chem} = -0.293\%$ is marked by the arrow, which is the origin for K_s. For a spin-triplet state with a cubic crystal structure, a reduction $K_s/3$ is expected, whose position is marked by the arrow at $K = -0.217\%$. Clearly, $K - K_{dia}$ at $T = 0$ goes far below this position. In fact, $K_s(T = 0)/K_s(T = T_c) = 0.36 \pm 0.10$ is found. Namely, the reduction is about two-thirds of the total spin Knight shift. This result indicates that a spin-singlet superconducting state is realized in the polycrystalline sample of $Sn_{0.96}In_{0.04}Te$ studied here.

IV. DISCUSSION

We make a few comments on the results and the connection to topological superconductivity seen in $Cu_xBi_2Se_3$. First, we note that even if we use the larger $\mu_0 H_{c2}(0) = 0.53$ T from the Werthamer-Helfand-Hohenberg fitting, our conclusion does not change. In this case, $K_{dia}(0) = -0.008\%$ and $K_s(0)/K_s(T_c) = 0.39 \pm 0.1$. Second, the finite K_s even at $T = 0$ can be explained by the scattering due to spin-orbit interaction [27], as seen in many BCS superconductors with

large spin-orbit coupling such as Sn and Hg [28]. A finite K_s was also found in $Cu_xBi_2Se_3$ when the magnetic field was applied along the d-vector direction [8]. Third, the isotropic superconducting state found here is consistent with the quasilocalized impurity bound states due to In doping [13]. As the impurity bound state has no translational symmetry, a wave-number-independent gap is natural.

The results obtained in this work do not support the notion that the superconductivity in $Sn_{0.96}In_{0.04}Te$ is topological. For a material with spatial inversion and time-reversal symmetry, sufficient conditions for topological superconductivity have been established; namely, the parity of the wave function for electron pairs in the superconducting state is odd [6], and the Fermi surface encloses an odd number of time-reversal-invariant momenta [6]. These two conditions are fulfilled in $Cu_xBi_2Se_3$ [8,29].

The identification of spin-singlet superconductivity in this work suggests that the superconducting wave function of $Sn_{0.96}In_{0.04}Te$ has an even parity and hence it is likely to be a conventional, topologically trivial superconductor.

Quite often, surface-sensitive probes and bulk-sensitive probes such as NMR give different conclusions [8,30–32]. Sometimes the results are different even among surface-sensitive probes, as encountered in studies of $Cu_xBi_2Se_3$ [30–32]. The situation is also true for the current compound, for which unconventional superconductivity was previously suggested by point-contact spectroscopy [16]. We note that, as a consequence of the topological superconductivity in the bulk, a gapless edge state can appear in the surface which can be seen by surface-sensitive probes. However, the presence or absence of a signature for a surface state alone does not immediately indicate the properties of the bulk. This is because, in addition to the technical issues [32], the surface has additional complications.

Due to the broken inversion symmetry on the surface and the strong spin-orbit coupling, parity mixing occurs on the surface. Thus, even the bulk of $Cu_xBi_2Se_3$ has an odd-parity, s-wave component that can be seen on the surface [33]. The opposite situation, as in the case of $Sn_{1-x}In_xTe$, is also possible. In the present case, there is another possibility that may reconcile the different results of NMR and the previous point-contact spectroscopy [16]. That is, the sample purity is different in the two measurements. The sample used in the previous study is a single crystal and has less disorder [17], while the sample used in NMR has more disorder as evidenced by the extremely low residual-resistivity ratio ($\sim$1.3). It was reported previously that point-contact spectroscopy depends strongly on the degree of disorder of the samples [17]. In more disordered crystals, no zero-bias peak was observed [17].

V. CONCLUSION

In summary, we have performed ^{125}Te-NMR in polycrystalline samples of the doped TCI, $Sn_{1-x}In_xTe$. K_{chem} was determined to be -0.293% from the K-$(T_1T)^{-1/2}$ plot with various x's and determined the spin Knight shift K_s for the $x = 0.04$ sample. The FWHM of the ^{125}Te-NMR spectra of $Sn_{0.96}In_{0.04}Te$ was T independent below $0.5T_c$, which indicates a fully gapped superconducting state. $K_s(T = 0)/K_s(T = T_c)$ reached 0.36 ± 0.10, which is much smaller than the limiting value of 2/3 for a spin-triplet state in a polycrystal sample with a cubic crystal structure. These results indicate that the measured polycrystaline sample of $Sn_{0.96}In_{0.04}Te$ is a spin-singlet superconductor.

ACKNOWLEDGMENTS

We thank Z. Wang for the Hall coefficient measurements and S. Katsube, K. Segawa, and S. Kawasaki for help with some of the measurements and acknowledge partial support by MEXT Grant No. 15H05852 (Topological Materials Science) and JSPS Grants No. 16H0401618 and No. 17K14340, as well as by NSFC (Grant No. 11634015) and DFG (CRC1238 "Control and Dynamics of Quantum Materials"; Project A04).

[1] M. Z. Hasan and C. L. Kane, Rev. Mod. Phys. **82**, 3045 (2010).
[2] X.-L. Qi and S.-C. Zhang, Rev. Mod. Phys. **83**, 1057 (2011).
[3] T. H. Hsieh, H. Lin, J. Liu, W. Duan, A. Bansil, and L. Fu, Nat. Commun. **3**, 982 (2012).
[4] Y. Tanaka, Z. Ren, T. Sato, K. Nakayama, S. Souma, T. Takahashi, K. Segawa, and Y. Ando, Nat. Phys. **8**, 800 (2012).
[5] Y. Ando and L. Fu, Annu. Rev. Condens. Matter Phys. **6**, 361 (2015).
[6] L. Fu and E. Berg, Phys. Rev. Lett. **105**, 097001 (2010).
[7] M. Sato and Y. Ando, Rep. Prog. Phys. **80**, 076501 (2017).
[8] K. Matano, M. Kriener, K. Segawa, Y. Ando, and G.-q. Zheng, Nat. Phys. **12**, 852 (2016).
[9] Y. S. Hor, A. J. Williams, J. G. Checkelsky, P. Roushan, J. Seo, Q. Xu, H. W. Zandbergen, A. Yazdani, N. P. Ong, and R. J. Cava, Phys. Rev. Lett. **104**, 057001 (2010).
[10] J. K. Hulm, C. K. Jones, D. W. Deis, H. A. Fairbank, and P. A. Lawless, Phys. Rev. **169**, 388 (1968).
[11] P. B. Allen and M. L. Cohen, Phys. Rev. **177**, 704 (1969).
[12] A. S. Erickson, J.-H. Chu, M. F. Toney, T. H. Geballe, and I. R. Fisher, Phys. Rev. B **79**, 024520 (2009).
[13] S. Maeda, S. Katsube, and G.-q. Zheng, J. Phys. Soc. Jpn. **86**, 024702 (2017).
[14] A. L. Shelankov, Solid State Commun. **62**, 327 (1987).
[15] N. Haldolaarachchige, Q. Gibson, W. Xie, M. B. Nielsen, S. Kushwaha, and R. J. Cava, Phys. Rev. B **93**, 024520 (2016).
[16] S. Sasaki, Z. Ren, A. A. Taskin, K. Segawa, L. Fu, and Y. Ando, Phys. Rev. Lett. **109**, 217004 (2012).
[17] M. Novak, S. Sasaki, M. Kriener, K. Segawa, and Y. Ando, Phys. Rev. B **88**, 140502(R) (2013).
[18] L. P. He, Z. Zhang, J. Pan, X. C. Hong, S. Y. Zhou, and S. Y. Li, Phys. Rev. B **88**, 014523 (2013).
[19] M. Saghir, J. A. T. Barker, G. Balakrishnan, A. D. Hillier, and M. R. Lees, Phys. Rev. B **90**, 064508 (2014).
[20] T. Hashimoto, K. Yada, M. Sato, and Y. Tanaka, Phys. Rev. B **92**, 174527 (2015).
[21] R. D. Zhong, J. A. Schneeloch, X. Y. Shi, Z. J. Xu, C. Zhang, J. M. Tranquada, Q. Li, and G. D. Gu, Phys. Rev. B **88**, 020505(R) (2013).
[22] N. R. Werthamer, K. Helfand, and P. C. Hohenberg, Phys. Rev. **147**, 295 (1966).

[23] E. H. Brandt, Phys. Rev. B **37**, 2349 (1988).
[24] P. G. de Gennes, *Superconductivity of Metals and Alloys* (Westview Press, Oxford, UK, 1999).
[25] G. Du, Z. Du, D. Fang, H. Yang, R. D. Zhong, J. Schneeloch, G. D. Gu, and H.-H. Wen, Phys. Rev. B **92**, 020512(R) (2015).
[26] G.-q. Zheng, H. Ozaki, Y. Kitaoka, P. Kuhns, A. P. Reyes, and W. G. Moulton, Phys. Rev. Lett. **88**, 077003 (2002).
[27] J. Appel, Phys. Rev. **139**, A1536 (1965).
[28] D. E. MacLaughlin, Solid State Phys. **31**, 1 (1976).
[29] Y. Xia, D. Qian, D. Hsieh, L. Wray, A. Pal, H. Lin, A. Bansil, D. Grauer, Y. S. Hor, R. J. Cava, and M. Z. Hasan, Nat. Phys. **5**, 398 (2009).
[30] S. Sasaki, M. Kriener, K. Segawa, K. Yada, Y. Tanaka, M. Sato, and Y. Ando, Phys. Rev. Lett. **107**, 217001 (2011).
[31] N. Levy, T. Zhang, J. Ha, F. Sharifi, A. A. Talin, Y. Kuk, and J. A. Stroscio, Phys. Rev. Lett. **110**, 117001 (2013).
[32] H. B. Peng, D. De, B. Lv, F. Wei, and C.-W. Chu, Phys. Rev. B **88**, 024515 (2013).
[33] T. Mizushima, A. Yamakage, M. Sato, and Y. Tanaka, Phys. Rev. B **90**, 184516 (2014).